Nanoscale Research Letters
a SpringerOpen Journal

NANO EXPRESS Open Access

A nontoxic and low-cost hydrothermal route for synthesis of hierarchical Cu_2ZnSnS_4 particles

Yu Xia[1,3], Zhihong Chen[2], Zhengguo Zhang[2], Xiaoming Fang[2*] and Guozheng Liang[1*]

Abstract

We explore a facile and nontoxic hydrothermal route for synthesis of a Cu_2ZnSnS_4 nanocrystalline material by using L-cysteine as the sulfur source and ethylenediaminetetraacetic acid (EDTA) as the complexing agent. The effects of the amount of EDTA, the mole ratio of the three metal ions, and the hydrothermal temperature and time on the phase composition of the obtained product have been systematically investigated. The addition of EDTA and an excessive dose of $ZnCl_2$ in the hydrothermal reaction system favor the generation of kesterite Cu_2ZnSnS_4. Pure kesterite Cu_2ZnSnS_4 has been synthesized at 180°C for 12 h from the reaction system containing 2 mmol of EDTA at 2:2:1 of Cu/Zn/Sn. It is confirmed by Raman spectroscopy that those binary and ternary phases are absent in the kesterite Cu_2ZnSnS_4 product. The kesterite Cu_2ZnSnS_4 material synthesized by the hydrothermal process consists of flower-like particles with 250 to 400 nm in size. It is revealed that the flower-like particles are assembled from single-crystal Cu_2ZnSnS_4 nanoflakes with *ca.* 20 nm in size. The band gap of the Cu_2ZnSnS_4 nanocrystalline material is estimated to be 1.55 eV. The films fabricated from the hierarchical Cu_2ZnSnS_4 particles exhibit fast photocurrent responses under intermittent visible-light irradiation, implying that they show potentials for use in solar cells and photocatalysis.

Keywords: Cu_2ZnSnS_4; Nanocrystalline material; Hierarchical particles; Hydrothermal process; Photoelectrochemical property

Background

The quaternary Cu_2ZnSnS_4 (CZTS) compound, derived from $CuInS_2$ by replacing In(III) with Zn(II) and Sn(IV), has the advantages of optimum direct band gap (around 1.5 eV) for use in single-junction solar cells, abundance of the constituent elements, and high absorption coefficient (>10^4 cm^{-1}) [1-5]. Thus, increasing attention has been paid on CZTS materials in recent years [6-10]. Low-cost solar cells based on CZTS films as absorber layers have achieved an increasing conversion efficiency [11-15]. CZTS nanocrystalline materials have been found to show potentials for use in negative electrodes for lithium ion batteries [16] and counter electrodes for high-efficiency dye-sensitized solar cells [17-19] and as novel photocatalysts for hydrogen production [20]. Obviously, an environment-friendly and low-cost synthesis route for the large-scale production of CZTS in high quality is an essential prerequisite for its applications in all those fields.

At present, the routes for synthesis of CZTS nanocrystalline materials can be subsumed under two broad categories: the hot-injection method [12,21-23] and the solvothermal process [13,18,24-26]. Although the hot-injection method can be used to synthesize CZTS nanocrystals with narrow size distribution, this method suffers from several shortcomings such as the need of expensive raw materials with high levels of toxicity, complicated processes, and high reaction temperatures (above 250°C). In contrast with the hot-injection method, the solvothermal process, which usually produces hierarchical CZTS particles by one-pot reaction, possesses the advantages of simple process and relative cheap raw materials. Furthermore, it has been found that hierarchical particles can provide a large surface area along with the functions of generating light scattering and favoring electron transport, as compared with nanocrystals [13]. Up to now, anhydrous ethylenediamine [24,26], the mixture of ethylenediamine and water [27-29], ethylene glycol [13,18], triethylene glycol [18], and dimethyl formamide (DMF) [30] have been used as a solvent for the solvothermal method, respectively. In

* Correspondence: cexmfang@scut.edu.cn; lgzheng@suda.edu.cn
[2]Key Laboratory of Enhanced Heat Transfer and Energy Conservation, Ministry of Education, School of Chemistry and Chemical Engineering, South China University of Technology, Guangzhou 510640, China
[1]Jiangsu Key Laboratory of Advanced Functional Polymer Design and Application, College of Chemistry, Chemical Engineering, and Materials Science, Soochow University, Suzhou 215123, China
Full list of author information is available at the end of the article

contrast with those organic solvents, water is much cheaper and more environment-friendly. Undoubtedly, if water is used to replace these organic solvents, a hydrothermal route will be developed, which is more desirable for the environment-friendly and low-cost synthesis of CZTS nanocrystalline materials. However, few investigations on synthesis of CZTS nanocrystalline materials by the hydrothermal method have been reported, except the hydrothermal reactions with Na_2S [31] or thiourea [32] as the sulfur source. Note that selecting a suitable sulfur source is important for exploring a green hydrothermal process for preparing CZTS nanocrystalline materials. It has been reported that H_2S is usually generated as a toxic and corrosive intermediate product from the reaction systems containing sulfur, Na_2S, or thiourea as the sulfur source [33]. Different from those sulfur sources, L-cysteine has been used to prepare metal sulfide nanomaterials without the generation of H_2S as a by-product [30]. Thus, in the current work, by the aid of ethylenediaminetetraacetic acid (EDTA) as a complexing agent, a low-cost and nontoxic hydrothermal route for synthesis of CZTS has been developed by using water as the solvent and L-cysteine as the sulfur source. The effects of the amount of EDTA, the mole ratio of the three metal ions, and the hydrothermal temperature and time on the phase composition of the obtained samples have been systematically investigated. The phase composition of the obtained CZTS sample has been further confirmed by Raman spectrometry. The microstructure and morphology of the pure CZTS sample have been characterized, and its optical absorption property has been examined. Moreover, the prepared CZTS nanocrystalline material has been employed to fabricate films, and the photoelectrochemical property of the obtained films has been evaluated.

Methods

Synthesis of CZTS

$CuCl_2 \cdot 2H_2O$, $ZnCl_2$, $SnCl_2 \cdot 2H_2O$, L-cysteine, and EDTA were of analytical grade and used as received without further purification. In a typical synthesis, 2 mmol $CuCl_2 \cdot 2H_2O$, 2 mmol of $ZnCl_2$, 1 mmol of $SnCl_2 \cdot 2H_2O$, 4 mmol of L-cysteine, and 0 to 3 mmol of EDTA were dispersed in 20 ml of deionized water for 5 min under constant stirring, and then the obtained solution was transferred to an acid digestion bomb (50 ml). The hydrothermal synthesis was conducted at 170°C to 190°C for 6 to 16 h in an electric oven. After synthesis, the bomb was cooled down naturally to room temperature. The final product was filtrated and washed with 30% and 80% ethanol, followed by drying at 60°C in a vacuum oven. Moreover, in order to investigate the mole ratio of the three metal ions (Cu/Zn/Sn) in the reaction system on the phase composition of the obtained product, three samples were synthesized at 2:1:1, 2:2:1, and 2:3:1 of Cu/Zn/Sn, respectively.

Characterizations

Powder X-ray diffraction (PXRD) patterns of samples were performed on a Bruker D8 ADVANCE diffraction system (Bruker AXS GmbH, Karlsruhe, Germany) using Cu Kα radiation ($\lambda = 1.5406$ Å), operated at 40 kV and 40 mA with a step size of 0.02°. The morphology of the pure CZTS sample was observed by using a scanning electron microscope (SEM, Nova Nano 430, FEI, Holland). Transmission electron microscopy (TEM) and high-resolution transmission electron microscopy (HRTEM) images were obtained by using a JEOL JEM-2100 F field emission electron microscope (JEOL Ltd., Akishima, Tokyo, Japan). The Raman spectrum of the sample was recorded on a microscopic Raman spectrometer (LabRAM Aramis, Horiba Jobin Yvon Inc., Edison, NJ, USA). The diffuse reflectance spectrum (DRS) of the CZTS sample was obtained by using a Shimadzu U-3010 spectrophotometer (Shimadzu Corporation, Nakagyo-ku, Kyoto, Japan) equipped with an integrating sphere assembly.

Photoelectrochemical measurement

The prepared CZTS sample was used to fabricate films as follows: 0.05 g of the sample was mixed with ethanol followed by ultrasound. The obtained CZTS 'ink' was then coated onto indium-tin (ITO) oxide glass by spin coating for several times, followed by drying at 120°C for 1 h. Photoelectrochemical measurements were conducted on the obtained CZTS films. Photocurrents were measured on an electrochemical analyzer (CorrTest CS350, CorrTest Instrument Co., Wuhan, China) in a standard three-electrode system by using the prepared CZTS film as the working electrode, a Pt flake as the counter electrode, and Ag/AgCl as the reference electrode. A 300-W Xe lamp served as a light source, and 0.5 M Na_2SO_4 solution was used as the electrolyte.

Results and discussion

Effects of hydrothermal reaction conditions

Amount of EDTA

In order to investigate the amount of EDTA on the phase composition of the obtained product, several samples have been synthesized at 180°C for 16 h by adding different amounts of EDTA into the reaction system with Cu/Zn/Sn at 2:2:1. Figure 1 displays the PXRD patterns of the samples. The sample obtained from the reaction system containing no EDTA shows seven diffraction peaks located at 26.8°, 28.7°, 30.3°, 33.0°, 47.6°, 51.4°, and 56.4°. According to the standard PXRD pattern of kesterite CZTS (PDF no. 26-0575), the four diffraction peaks located at 28.7°, 33.0°, 47.6°, and 56.4° can be attributed to (112), (200), (220), and (312) planes of kesterite CZTS, respectively. Note that a new wurtzite phase of CZTS was discovered by Lu et al. [8] and that the arrangements of atoms in the simulated wurtzite were basically similar to those in

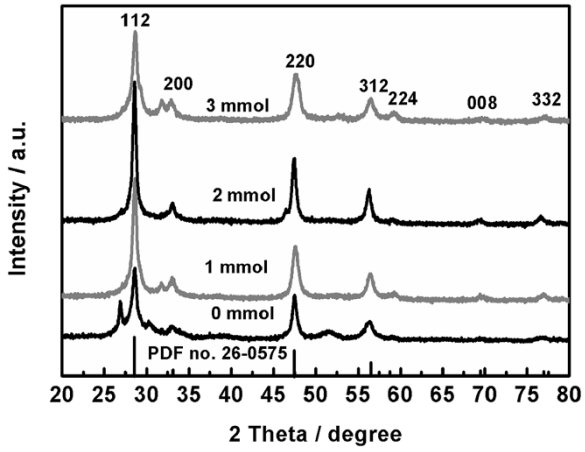

Figure 1 XRD patterns of the samples obtained under different amounts of EDTA.

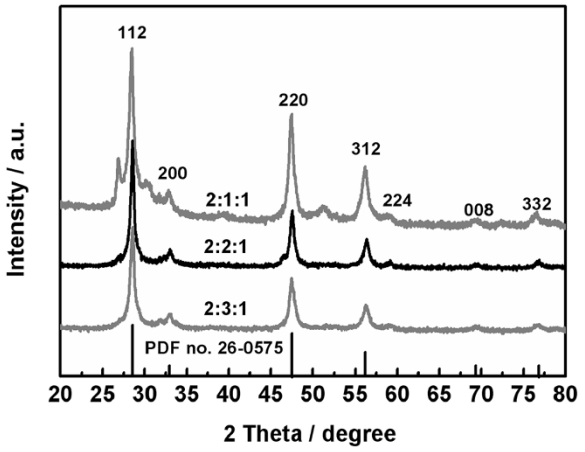

Figure 2 XRD patterns of the samples obtained at different Cu/Zn/Sn/S mole ratios.

kesterite [34]. Consequently, the three strongest peaks located at 28.7°, 47.6°, and 56.4° can be also ascribed to (002), (110), and (112) planes of wurtzite CZTS, respectively. Besides, the diffraction peaks located at 26.8°, 30.3°, and 51.4° can be attributed to (100), (101), and (103) planes of wurtzite CZTS, respectively. It is revealed that the CZTS sample prepared from the reaction system containing no EDTA is a mixture of kesterite and wurtzite. The presence of the diffraction peak located at 33.0°, originated from (200) planes of kesterite CZTS, along with the absence of the diffraction peak located at around 39°, corresponding to (102) planes of wurtzite CZTS, implies that the content of kesterite is more than that of wurtzite in the CZTS sample. After 1 mmol of EDTA has been added into the reaction system, the obtained sample exhibits four main diffraction peaks of kesterite CZTS, together with one weak impurity peak located at 31.6°, which probably originates from CuS or Sn_2S_3. The absence of the diffraction peaks of wurtzite CZTS suggests that the addition of EDTA in the hydrothermal reaction system hampers the formation of wurtzite, thus favoring the production of pure kesterite CZTS. Furthermore, the PXRD pattern of the sample produced from the reaction system containing 2 mmol of EDTA is identical to the standard one of kesterite CZTS. The relatively high intensity of the diffraction peaks implies that the obtained sample is in high purity and good crystallinity. However, as the amount of EDTA is further increased to 3 mmol, the obtained sample exhibits the diffraction peaks of kesterite CZTS, together with one weak impurity peak located at 31.6°. The above results suggest that a suitable amount of EDTA added into the reaction system is essential for producing pure kesterite CZTS by the hydrothermal process. For the solvothermal process with *N*,*N*-dimethylformamide (DMF) as the solvent, EDTA was not needed for preparing pure kesterite CZTS, even if L-cysteine was also used as the sulfur source [30]. The reason for this difference is possibly due to the fact that the complex reactions between the three metal ions with L-cysteine take place more easily in DMF than in water. As a result, EDTA is needed for the process with water as the solvent and L-cysteine as the sulfur source, which is used as a complexing agent. It is obvious that the hydrothermal process provides an environment-friendly and low-cost route for producing pure kesterite CZTS, as compared with the solvothermal method with DMF as the solvent.

Mole ratio of three metal ions

The stoichiometric control of quaternary compounds is complicated by the tendency of forming a plurality of compositional phases, due to the difference in reactivity of the cationic precursors. Consequently, the mole ratio of the three cationic precursors in the reaction system should have an important effect on the phase composition of the

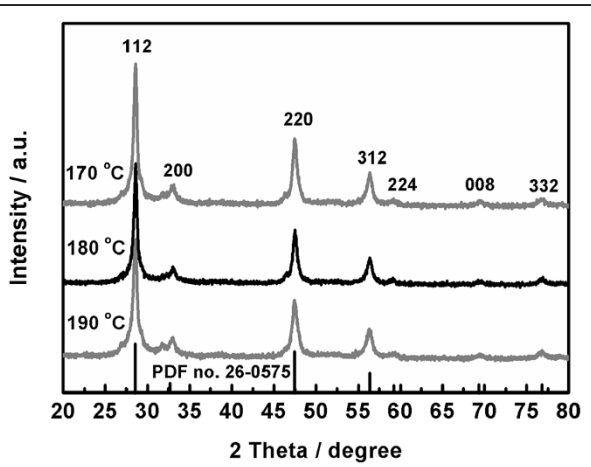

Figure 3 XRD patterns of the samples obtained at different hydrothermal temperatures.

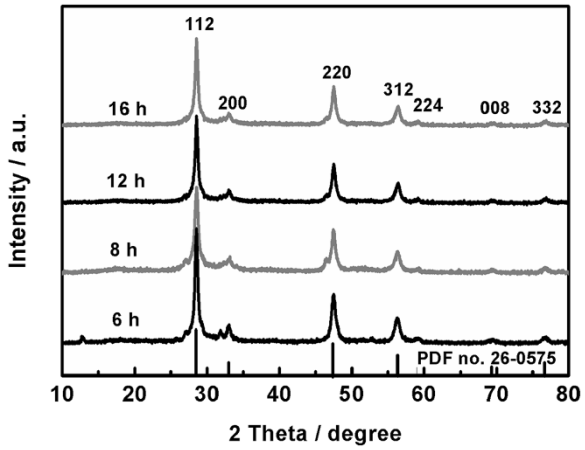

Figure 4 XRD patterns of the samples obtained at 180°C for different times.

obtained samples. Figure 2 shows the PXRD patterns of the samples synthesized at 180°C for 16 h from the reaction system containing 2 mmol of EDTA at different mole ratios of the three metal ions. At Cu/Zn/Sn = 2:1:1, corresponding to the stoichiometric ratio of CZTS, the obtained sample shows a similar XRD pattern to the one prepared from the reaction system containing no EDTA (Figure 1), implying that it has a mixed phase of kesterite and wurtzite. Besides, a weak impurity peak located at 31.7° appears. As the amount of $ZnCl_2$ in the reaction system is doubled, and thus Cu/Zn/Sn is accordingly changed from 2:1:1 to 2:2:1, the obtained sample can be identified as kesterite CZTS in high purity and good crystallinity. Note that at Cu/Zn/Sn = 2:3:1, the obtained sample exhibits several diffraction peaks of kesterite CZTS, together with one weak impurity peak located at 31.8°. These results indicate that the mole ratio of the three cationic precursors influences the phase composition of the obtained product. An excessive dose of $ZnCl_2$ (double the stoichiometric ratio of Zn in CZTS) in the reaction system favors the production of pure kesterite CZTS.

Effect of hydrothermal temperature

With the amount of EDTA fixed at 2 mmol and Cu/Zn/Sn set at 2:2:1, the hydrothermal synthesis was conducted at different temperatures for 16 h. Figure 3 displays the PXRD patterns of the samples prepared at 170°C, 180°C, and 190°C. All the obtained samples show the seven diffraction peaks located 28.7°, 33.0°, 47.6°, 56.4°, 59.2°, 69.5°, and 76.7°, which are ascribed to (112), (200), (220), (312), (224), (008), and (332) planes of kesterite CZTS, respectively. However, the two samples prepared

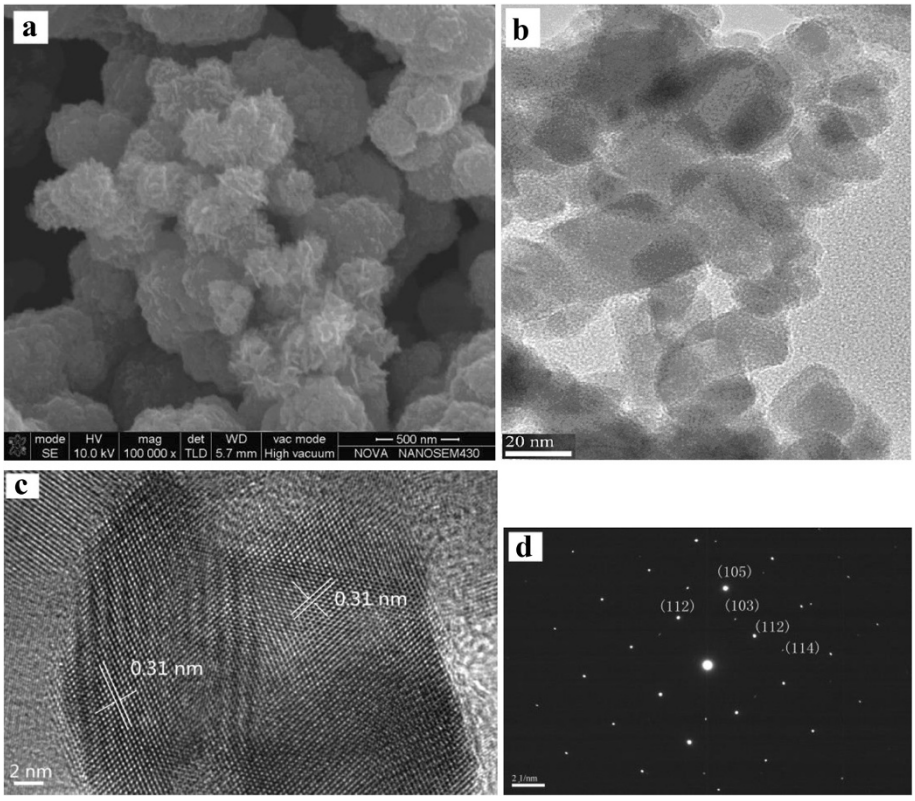

Figure 5 SEM, TEM, and HRTEM images and SAED pattern of the CZTS sample prepared by hydrothermal method. (a) SEM, **(b)** TEM, **(c)** HRTEM, and **(d)** SAED pattern.

at 170°C and 190°C exhibit one weak impurity peak located at 31.8°. It is suggested that kesterite CZTS can be synthesized at the hydrothermal temperatures ranging between 170°C and 190°C from the reaction system containing 2 mmol of EDTA at 2:2:1 of Cu/Zn/Sn. The suitable temperature for producing pure kesterite CZTS should be around 180°C.

Effect of reaction time

In order to investigate the effect of the reaction time on the phase composition of the obtained product, four samples have been synthesized at 180°C for 16, 12, 8, and 6 h, respectively, and their PXRD patterns are displayed in Figure 4. As the reaction time is reduced from 16 to 12 h, the obtained sample still has the phase of kesterite in high purity and good crystallinity. However, as the reaction time is further reduced to 8 and 6 h, the obtained two samples show the weak impurity peaks located at 46.5° and 31.8°, respectively. These results imply that pure kesterite CZTS can be produced by the hydrothermal process at 180°C for no less than 12 h.

Microstructure, morphology, and optical absorption property

Figure 5 shows SEM, TEM, and HRTEM images and a SAED pattern of the pure CZTS sample synthesized at 180°C for 12 h from the reaction system containing 2 mmol of EDTA at 2:2:1 of Cu/Zn/Sn. The SEM image (Figure 5a) reveals general morphologies of flower-like particles, which are assembled from nanoflakes. The sizes of the hierarchical particles range from 250 to 400 nm, much smaller than the microspheres (approximately 2.2 μm) prepared by the solvothermal method at 250°C for 8 h [18]. The observations of the CZTS sample by TEM and HRTEM were performed after it had been dispersed into ethanol by ultrasound. The TEM image (Figure 5b) shows some hexagonal nanoflakes with *ca.* 20 nm in size, implying that the hierarchical CZTS particles have been disassembled into the nanoflakes by ultrasound. As shown from the HRTEM image (Figure 5c), the continuous lattice fringes throughout a particle indicate the single crystalline nature of the nanoscale flakes, which is further confirmed by the dotted SAED pattern recorded for a single particle (Figure 5d). The *d*-spacing value has been calculated to be 0.31 nm (Figure 5c), identical to the theoretical value of 0.31 nm for (112) planes of kesterite CZTS.

Some binary and ternary compounds including ZnS, Cu_3SnS_4, and Cu_2SnS_3 could be present as impurity in CZTS [35], and their PXRD patterns are similar to that of kesterite CZTS. As a result, it is hard to distinguish CZTS from those binary and ternary compounds by using XRD. In order to further confirm the phase composition of the hierarchical CZTS particles, room-temperature Raman spectroscopy has been employed due to the ability of this technique to distinguish between the CZTS phase and the ZnS, Cu_3SnS_4, and Cu_2SnS_3 phases. Figure 6 shows the room-temperature Raman spectrum of the hierarchical

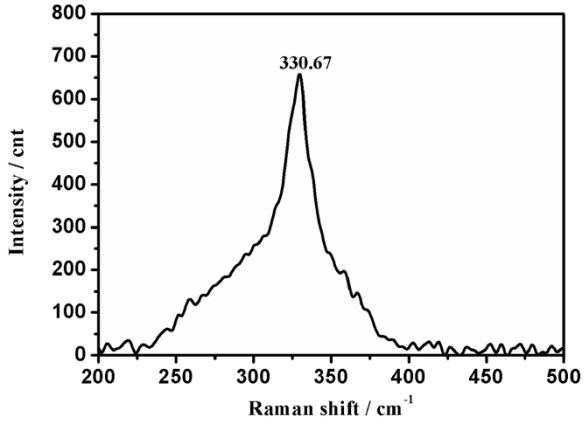

Figure 6 The room-temperature Raman spectrum of the hierarchical CZTS flower-like particles.

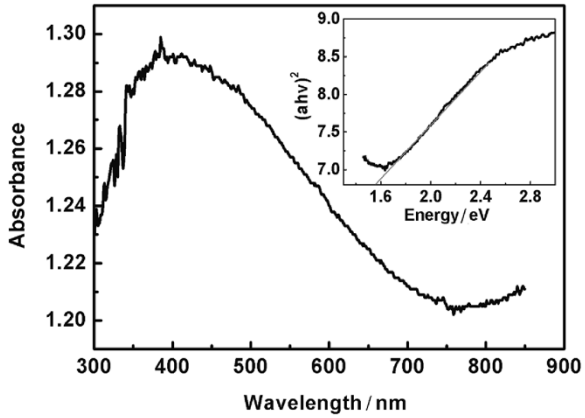

Figure 7 The UV-vis diffuse reflectance spectrum of the hierarchical CZTS flower-like particles.

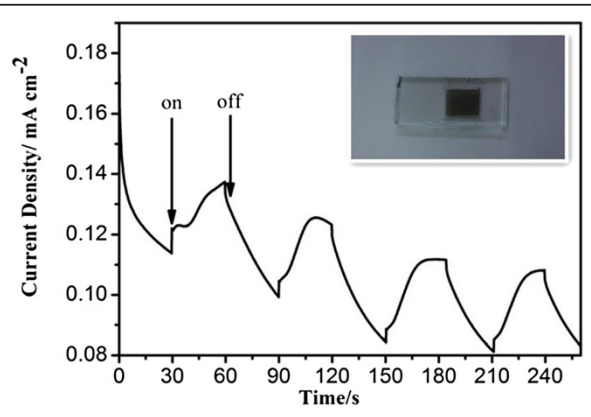

Figure 8 The transient photocurrent responses (*I-t*) of the CZTS film at 0.5 V vs. Ag/AgCl.

CZTS particles. The kesterite CZTS sample exhibits a high intensity peak at 330.67 cm^{-1}, close to the reported Raman intense peak positions in the range from 331 to 338 cm^{-1} for kesterite CZTS and totally different from the characteristic peaks of the ZnS (351 cm^{-1}), Cu_3SnS_4 (318 cm^{-1}), and Cu_2SnS_3 (298 cm^{-1}) phases. It can be inferred that those impurity phases are absent in the kesterite CZTS sample.

Figure 7 shows the optical absorption spectrum obtained from diffuse reflectance of the hierarchical CZTS particles. The direct optical band gap of the CZTS particles has been calculated from the UV-vis spectrum to be 1.55 eV by extrapolation of the linear region of a plot of $(\alpha hv)^2$ versus energy (the inset in Figure 7), where α represents the absorption coefficient and hv is the photon energy. Compared to 1.48 eV of bulk CZTS, a blueshift of 0.07 eV in the band gap is observed for the hierarchical CZTS particles, which could be attributed to the quantum confinement effect originated from the CZTS single-crystal nanoflakes.

Photoelectrochemical property of CZTS films

The hierarchical CZTS particles have been employed to fabricate films, and the photoelectrochemical property of the obtained CZTS films has been evaluated by measuring their transient current response (*I-t*) with several on-off cycles. Figure 8 shows the photoelectrochemical *I-t* curve of the CZTS film under intermittent visible-light irradiation (>420 nm) at 0.5 V vs Ag/AgCl, and a typical photograph of the film is inserted in this figure. The CZTS film exhibits fast photocurrent responses, indicating its good photoelectrochemical property. It can be suggested that the hierarchical CZTS particles synthesized by the facile and nontoxic hydrothermal route show potentials for use in solar cells and photocatalysis.

Conclusions

The reaction conditions including the amount of EDTA, the mole ratio of the three metal ions, and the hydrothermal temperature and time have an important effect on the phase composition of the obtained product. A suitable amount of EDTA is needed for synthesis of pure kesterite CZTS by the hydrothermal process with L-cysteine as the sulfur source. An excessive dose of $ZnCl_2$ (double the stoichiometric ratio of Zn in CZTS) in the reaction system favors the production of kesterite CZTS. Pure kesterite CZTS can be produced by the hydrothermal process at 180°C for no less than 12 h. It is confirmed that those binary and ternary phases are absent in the kesterite CZTS product. The kesterite CZTS material synthesized by the hydrothermal process consists of flower-like particles with 250 to 400 nm in size. The particles are assembled from the single-crystal CZTS nanoflakes with *ca.* 20 nm in size. The band gap of the CZTS material is estimated to be 1.55 eV. The CZTS films fabricated from the flower-like CZTS particles exhibit fast photocurrent responses, making them show potentials for use in solar cells and photocatalysis.

Competing interests

The authors declare that they have no competing interests.

Authors' contributions

YX designed and conducted the experiments, carried out the experimental analyses, and drafted the manuscript. ZC fabricated the films and performed the photoelectrochemical measurement. ZZ, XF, and GL conceived the study, participated in its design and coordination, wrote the introduction, and modified the manuscript. All authors read and approved the final manuscript.

Acknowledgements

This work is supported by the National Natural Science Foundation of China (60976053 and 21276088).

Author details

[1]Jiangsu Key Laboratory of Advanced Functional Polymer Design and Application, College of Chemistry, Chemical Engineering, and Materials Science, Soochow University, Suzhou 215123, China. [2]Key Laboratory of Enhanced Heat Transfer and Energy Conservation, Ministry of Education, School of Chemistry and Chemical Engineering, South China University of Technology, Guangzhou 510640, China. [3]Suzhou Jufeng Electrical Insulation System Co. Ltd, Suzhou 215214, China.

Received: 8 January 2014 Accepted: 18 April 2014
Published: 4 May 2014

References

1. Ramasamy K, Malik MA, O'Brien P: **Routes to copper zinc tin sulfide Cu_2ZnSnS_4 a potential material for solar cells.** *Chem Commun* 2012, **48**(46):5703–5714.
2. Fairbrother A, García-Hemme E, Izquierdo-Roca V, Fontané X, Pulgarín-Agudelo FA, Vigil-Galán O, Pérez-Rodríguez A, Saucedo E: **Development of a selective chemical etch to improve the conversion efficiency of Zn-rich Cu_2ZnSnS_4 solar cells.** *J Am Chem Soc* 2012, **134**(19):8018–8021.
3. Chen SY, Walsh A, Gong XG, Wei SH: **Classification of lattice defects in the kesterite Cu_2ZnSnS_4 and $Cu_2ZnSnSe_4$ earth-abundant solar cell absorbers.** *Adv Mater* 2013, **25**(11):1522–1539.
4. Paier J, Asahi R, Nagoya A, Kresse G: **Cu_2ZnSnS_4 as a potential photovoltaic material: a hybrid Hartree-Fock density functional theory study.** *Phys Rev B* 2009, **79**(11):115126.
5. Mitzi DB, Gunawan O, Todorov TK, Wang K, Guha S: **The path towards a high-performance solution-processed kesterite solar cell.** *Sol Energy Mater Sol Cells* 2011, **95**(6):1421–1436.
6. Shavel A, Cadavid D, Ibanez M, Carrete A, Cabot A: **Continuous production of Cu_2ZnSnS_4 nanocrystals in a flow reactor.** *J Am Chem Soc* 2012, **134**(3):1438–1441.
7. Walsh A, Chen SY, Wei SH, Gong XG: **Kesterite thin-film solar cells: advances in materials modelling of Cu_2ZnSnS_4.** *Adv Energy Mater* 2012, **2**(4):400–409.
8. Lu XT, Zhuang ZB, Peng Q, Li YD: **Wurtzite Cu_2ZnSnS_4 nanocrystals: a novel quaternary semiconductor.** *Chem Commun* 2011, **47**(11):3141–3143.
9. Khare A, Wills AW, Ammerman LM, Norris DJ, Aydil ES: **Size control and quantum confinement in Cu_2ZnSnS_4 nanocrystals.** *Chem Commun* 2011, **47**(42):11721–11723.
10. Zhang W, Zhai LL, He N, Zou C, Geng XZ, Cheng LJ, Dong YQ, Huang SM: **Solution-based synthesis of wurtzite Cu_2ZnSnS_4 nanoleaves introduced by alpha-Cu_2S nanocrystals as a catalyst.** *Nanoscale* 2013, **5**(17):8114–8121.
11. Guo Q, Ford GM, Yang WC, Walker BC, Stach EA, Hillhouse HW, Agrawal R: **Fabrication of 7.2% efficient CZTSSe solar cells using CZTS nanocrystals.** *J Am Chem Soc* 2010, **132**(49):17384–17386.
12. Guo QJ, Hillhouse HW, Agrawal R: **Synthesis of Cu_2ZnSnS_4 nanocrystal ink and its use for solar cells.** *J Am Chem Soc* 2009, **131**(33):11672–11673.

13. Zhou YL, Zhou WH, Li M, Du YF, Wu SX: **Hierarchical Cu_2ZnSnS_4 particles for a low-cost solar cell: morphology control and growth mechanism.** *J Phys Chem C* 2011, **115**(40):19632–19639.
14. Tian QW, Xu XF, Han LB, Tang MH, Zou RJ, Chen ZG, Yu MH, Yang JM, Hu JQ: **Hydrophilic Cu_2ZnSnS_4 nanocrystals for printing flexible, low-cost and environmentally friendly solar cells.** *Crystengcomm* 2012, **14**(11):3847–3850.
15. Wang J, Xin XK, Lin ZQ: **Cu_2ZnSnS_4 nanocrystals and graphene quantum dots for photovoltaics.** *Nanoscale* 2011, **3**(8):3040–3048.
16. Yin XS, Tang CH, Chen MH, Adams S, Wang H, Gong H: **Hierarchical porous Cu_2ZnSnS_4 films for high-capacity reversible lithium storage applications.** *J Mater Chem A* 2013, **1**(27):7927–7932.
17. Xin XK, He M, Han W, Jung JH, Lin ZQ: **Low-cost copper zinc tin sulfide counter electrodes for high-efficiency dye-sensitized solar cells.** *Angew Chem Int Ed* 2011, **50**(49):11739–11742.
18. Xu J, Yang X, Yang QD, Wong TL, Lee CS: **Cu_2ZnSnS_4 hierarchical microspheres as an effective counter electrode material for quantum dot sensitized solar cells.** *J Phys Chem C* 2012, **116**(37):19718–19723.
19. Dai PC, Zhang G, Chen YC, Jiang HC, Feng ZY, Lin ZJ, Zhan JH: **Porous copper zinc tin sulfide thin film as photocathode for double junction photoelectrochemical solar cells.** *Chem Commun* 2012, **48**(24):3006–3008.
20. Wang L, Wang WZ, Sun SM: **A simple template-free synthesis of ultrathin Cu_2ZnSnS_4 nanosheets for highly stable photocatalytic H-2 evolution.** *J Mater Chem* 2012, **22**(14):6553–6555.
21. Riha SC, Parkinson BA, Prieto AL: **Solution-based synthesis and characterization of Cu_2ZnSnS_4 nanocrystals.** *J Am Chem Soc* 2009, **131**(34):12054.
22. Steinhagen C, Panthani MG, Akhavan V, Goodfellow B, Koo B, Korgel BA: **Synthesis of Cu_2ZnSnS_4 nanocrystals for use in low-cost photovoltaics.** *J Am Chem Soc* 2009, **131**(35):12554–12555.
23. Ou KL, Fan JC, Chen JK, Huang CC, Chen LY, Ho JH, Chang JY: **Hot-injection synthesis of monodispersed $Cu_2ZnSn(S_xSe_{1-x})_4$ nanocrystals: tunable composition and optical properties.** *J Mater Chem* 2012, **22**(29):14667–14673.
24. Shi L, Pei CJ, Xu YM, Li Q: **Template-directed synthesis of ordered single-crystalline nanowires arrays of Cu_2ZnSnS_4 and $Cu_2ZnSnSe_4$.** *J Am Chem Soc* 2011, **133**(27):10328–10331.
25. Zhou YL, Zhou WH, Du YF, Li M, Wu SX: **Sphere-like kesterite Cu_2ZnSnS_4 nanoparticles synthesized by a facile solvothermal method.** *Mater Lett* 2011, **65**(11):1535–1537.
26. Chen LJ, Chuang YJ: **Quaternary semiconductor derived and formation mechanism by non-vacuum route from solvothermal nanostructures for high-performance application.** *Mater Lett* 2013, **91**:372–375.
27. Jiang HC, Dai PC, Feng ZY, Fan WL, Zhan JH: **Phase selective synthesis of metastable orthorhombic Cu_2ZnSnS_4.** *J Mater Chem* 2012, **22**(15):7502–7506.
28. Liu WC, Guo BL, Wu XS, Zhang FM, Mak CL, Wong KH: **Facile hydrothermal synthesis of hydrotropic Cu_2ZnSnS_4 nanocrystal quantum dots: band-gap engineering and phonon confinement effect.** *J Mater Chem A* 2013, **1**(9):3182–3186.
29. Pal M, Mathews NR, Gonzalez RS, Mathew X: **Synthesis of Cu_2ZnSnS_4 nanocrystals by solvothermal method.** *Thin Solid Films* 2013, **535**:78–82.
30. Cai Q, Liang XJ, Zhong JS, Shao MG, Wang Y, Zhao XW, Xiang WD: **Synthesis and characterization of sphere-like Cu_2ZnSnS_4 nanocrystals by solvothermal method.** *Acta Phys -Chim Sin* 2011, **27**(12):2920–2926.
31. Kush P, Ujjain SK, Mehra NC, Jha P, Sharma RK, Deka S: **Development and properties of surfactant-free water-dispersible Cu_2ZnSnS_4 nanocrystals: a material for low-cost photovoltaics.** *ChemPhysChem* 2013, **14**(12):2793–2799.
32. Liu WC, Guo BL, Mak C, Li AD, Wu XS, Zhang FM: **Facile synthesis of ultrafine Cu_2ZnSnS_4 nanocrystals by hydrothermal method for use in solar cells.** *Thin Solid Films* 2013, **535**:39–43.
33. Yu SH, Shu L, Yang JA, Han ZH, Qian YT, Zhang YH: **A solvothermal decomposition process for fabrication and particle sizes control of Bi_2S_3 nanowires.** *J Mater Res* 1999, **14**(11):4157–4162.
34. Li M, Zhou W-H, Guo J, Zhou Y-L, Hou Z-L, Jiao J, Zhou ZJ, Du ZL, Wu SX: **Synthesis of pure metastable wurtzite CZTS nanocrystals by facile one-pot method.** *J Phys Chem C* 2012, **116**(50):26507–26516.
35. Nagoya A, Asahi R, Wahl R, Kresse G: **Defect formation and phase stability of Cu_2ZnSnS_4 photovoltaic material.** *Phys Rev B* 2010, **81**(11):113202.

doi:10.1186/1556-276X-9-208
Cite this article as: Xia *et al.*: A nontoxic and low-cost hydrothermal route for synthesis of hierarchical Cu_2ZnSnS_4 particles. *Nanoscale Research Letters* 2014 **9**:208.